Cell, Vol. 85, 733–744, May 31, 1996, Copyright ©1996 by Cell Press

# A Syndrome of Multiorgan Hyperplasia with Features of Gigantism, Tumorigenesis, and Female Sterility in p27$^{Kip1}$-Deficient Mice

**Matthew L. Fero,* Michael Rivkin,‡ Michael Tasch,‖ Peggy Porter,† Catherine E. Carow,§ Eduardo Firpo,* Kornelia Polyak,# Li-Huei Tsai,‡ Virginia Broudy,§ Roger M. Perlmutter,‖ Kenneth Kaushansky,§ and James M. Roberts***

*Department of Basic Sciences
†Program in Cancer Biology
Division of Public Health
Fred Hutchinson Cancer Research Center
1124 Columbia Street
Seattle, Washington 98104
‡Department of Pathology
Harvard Medical School
Boston, Massachusetts, 02115
§Hematology Division
Department of Medicine
‖Howard Hughes Medical Institute
and Departments of Immunology, Biochemistry, and Medicine
University of Washington
Seattle, Washington 98195
#Howard Hughes Medical Institute
Johns Hopkins Oncology Center
Baltimore, Maryland 21231

## Summary

**Targeted disruption of the murine p27$^{Kip1}$ gene caused a gene dose–dependent increase in animal size without other gross morphologic abnormalities. All tissues were enlarged and contained more cells, although endocrine abnormalities were not evident. Thymic hyperplasia was associated with increased T lymphocyte proliferation, and T cells showed enhanced IL-2 responsiveness in vitro. Thus, p27 deficiency may cause a cell-autonomous defect resulting in enhanced proliferation in response to mitogens. In the spleen, the absence of p27 selectively enhanced proliferation of hematopoietic progenitor cells. p27 deletion, like deletion of the *Rb* gene, uniquely caused neoplastic growth of the pituitary pars intermedia, suggesting that p27 and Rb function in the same regulatory pathway. The absence of p27 also caused an ovulatory defect and female sterility. Maturation of secondary ovarian follicles into corpora lutea, which express high levels of p27, was markedly impaired.**

## Introduction

p27$^{Kip1}$ is one member of a new class of regulatory proteins that control cell cycle progression by binding to and inactivating cyclin–cyclin-dependent kinase (CDK) complexes (reviewed by Roberts et al., 1994; Sherr and Roberts, 1995). p27 was initially discovered as a CDK-inhibitory activity induced by extracellular anti-mitogenic signals (Koff et al., 1993; Polyak et al., 1994a; Firpo et al., 1994; Slingerland et al., 1994) and was purified and ultimately cloned by virtue of its ability to bind directly to the cyclin–CDK holoenzyme (Polyak et al., 1994b; Toyoshima and Hunter, 1994).

In mammals there are two known groups of CDK-inhibitory proteins: the INK4 proteins, which are specific inhibitors of the cyclin D–CDK4/CDK6 kinases (Xiong et al., 1993b; Serrano et al., 1993) and the Kip/Cip inhibitors. The Kip/Cip family contains p27, p21$^{Cip1/Waf1}$ (El-Diery et al., 1993; Gu et al., 1993; Harper et al., 1993; Xiong et al., 1993a, 1993b; Noda et al., 1994), and p57$^{Kip2}$ (Lee et al., 1995; Matsuoka et al., 1995). This family is defined by a conserved amino-terminal domain that is sufficient for both stable binding to cyclin–CDK complexes and inhibition of CDK protein kinase activity. The Kip/Cip proteins can inhibit each of the cyclin–CDK complexes essential for G1 progression and S phase entry. The promiscuous CDK-inhibitory activity of p21, p27, and p57 is reflected in their ability to cause cell cycle arrest when overexpressed in all cell types tested to date.

Apart from their homologous CDK-inhibitory domain, the Kip/Cip proteins have divergent structural and functional properties, which suggests that they might each have unique biological activities. p21, p27, and p57 are most divergent in their carboxy-terminal halves. It is through this portion of the protein that p21 directly binds to the replication protein, proliferating cell nuclear antigen (PCNA), and thereby inhibits its replicative activity (Flores-Rozas et al., 1994; Waga et al., 1994; Luo et al., 1995). In fact, the majority of cyclin–CDK molecules in proliferating, nontransformed cells are assembled into heteromeric complexes containing stoichiometric amounts of both p21 and PCNA (Xiong et al., 1993b). Neither p27 nor p57 binds to PCNA (Luo et al., 1995); what proteins, if any, bind to their carboxy-terminal domains remains to be determined.

In addition to their structural differences, the Kip/Cip inhibitors can also be distinguished by their unique responses to different mitogenic and anti-mitogenic signals. Various physiological states of cell cycle arrest are associated with elevated amounts of CDK inhibitors. For instance, p21 expression is increased in a p53-dependent manner in cells containing damaged DNA and independently of p53 in postmitotic, terminally differentiated cells (El-Diery et al., 1993; Deng et al., 1995; Brugarolas et al., 1995; Halevy et al., 1995; Parker et al., 1995). p27 expression, on the other hand, primarily increases in response to extracellular anti-proliferative signals. Normal cells grown to high cell density or deprived of serum mitogens undergo cell cycle arrest and express elevated levels of p27 protein (Firpo et al., 1994; Nourse et al., 1994; Coats et al., 1996). Moreover, cells exposed to anti-mitogenic factors like cAMP and rapamycin also express elevated levels of p27 (Kato et al., 1994; Nourse et al., 1994), and p27 cooperates with p15 (an INK4 family member) to cause G1 arrest in cells treated with transforming growth factor β (Reynisdottir et al., 1995). Thus, p27 might be an essential element in pathways that connect mitogenic signals to the cell cycle at the G1 restriction point. Indeed, cyclin–CDK complexes are catalytically inactive and quantitatively associated with

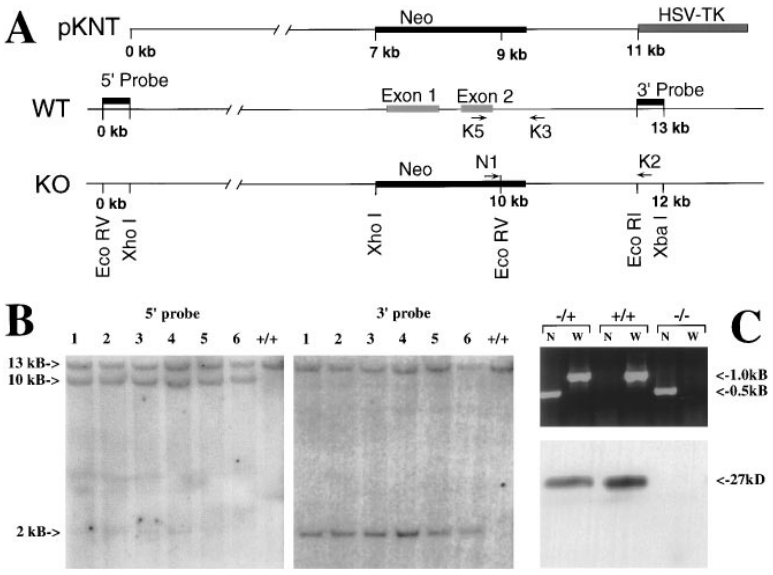


Figure 1. Targeted Disruption of the p27$^{Kip1}$ Gene

(A) Diagrams of the murine p27$^{Kip1}$ gene (WT), the targeting vector pKNT, and the predicted recombinant allele (knockout [KO]). Shown are the genomic DNA regions used as probes to identify homologous recombinants between pKNT and the p27$^{Kip1}$ gene. Also indicated are the sites of PCR primers used to distinguish the wild-type and disrupted p27 genes in ES cells and in DNA isolated from mice.

(B) Southern blots of ES cells containing a targeted disruption of the p27$^{Kip1}$ gene. Genomic DNA was digested with EcoRV plus XbaI and probed with the genomic DNA fragments indicated in (A).

(C) PCR analyses of genomic DNA from p27$^{+/+}$, p27$^{+/-}$, and p27$^{-/-}$ mice. The null allele, N, and wild-type allele, W, are amplified using primers N1 plus K3 and K5 plus K3, respectively. Also shown is an immunoblot of protein extracted from pituitaries of control, p27$^{+/-}$, and p27$^{-/-}$ mice.

p27 in cells deprived of serum mitogens. Furthermore, mitogen-starved fibroblasts cannot efficiently arrest at the G1 restriction point if p27 expression is blocked with p27 antisense oligonucleotides (Coats et al., 1996). To gain further insights into p27 function, we have used gene targeting to construct mice with a homozygous deletion of the p27 gene.

## Results

### Targeted Disruption of the p27$^{Kip1}$ Gene

The p27 gene in mouse and humans comprises two coding exons; there is also a third noncoding exon 3′ to the translation stop codon (Pietenpol et al., 1995). The vector used for targeted disruption of the p27 gene, pKNT, contained 7 kb of genomic DNA 5′ to exon 1 and 2 kb of DNA 3′ to exon 2 (Figure 1A). Homologous recombination between the targeting vector and the chromosome should replace the entire p27 coding region with the pgk–neo marker. Using polymerase chain reaction (PCR) to detect the presence of a genomic fragment unique to the predicted recombinant, it was shown that 15% of mouse embryonic stem (ES) cell clones had undergone a homologous recombination event between pKNT and the chromosomal p27 gene. Genomic blots using probes external to the targeting construct confirmed that both the 5′ and 3′ ends had recombined correctly (Figure 1B). Microinjection of C57/BL blastocysts with p27$^{+/-}$ ES cells produced multiple chimeric males, and transmission through the germline was demonstrated for chimeras derived from three ES cell clones. F1 generation p27 heterozygotes were interbred to produce F2 generation p27 nullizygous mice (Figure 1C). The complete absence of p27 or truncated forms of the protein was confirmed on immunoblots, and the levels appeared intermediate in p27 heterozygotes (Figure 1D).

### Growth and Viability of p27 Knockout Mice

Of the first 100 F2 progeny, 27 were p27$^{+/+}$, 49 were p27$^{+/-}$, and 24 were p27$^{-/-}$. This was consistent with a simple Mendelian pattern of inheritance and suggested that p27 deficiency did not result in significant mortality during embyrogenesis or fetal development. A cohort of 90 consecutive F2 generation p27 knockout, hemizygous, and control mice (all 129/Sv × C57/B6J hybrids) have been observed to 9 months of age. A single knockout mouse died from an invasive high grade thymic lymphoma at 6 months of age, but otherwise no fatalities have occurred. By this measure, p27-deficient mice were fully viable.

F2 generation p27$^{-/-}$ mice were significantly heavier than control littermates, and p27 heterozygotes were intermediate in size (Figures 2A, 2C, and 2D). The weight difference was slightly more pronounced in females and was roughly equivalent in inbred (129/Sv) and hybrid genetic backgrounds (data not shown). The weight difference was not evident at birth, became significant between 2 and 3 weeks of age, was maximal by 10 weeks of age, and was maintained throughout adulthood. (Figures 2C and 2D).

Apart from their increased size, p27-deficient mice were morphologically normal. At necropsy the mice did not have a disproportionate amount of body fat. The increased weight of the p27$^{-/-}$ mice was, at least in part, attributable to an enlargement of all internal organs (Figure 2B). Whereas most organs were increased in proportion to overall body weight, the thymus, spleen, and pituitary were disproportionately enlarged (see below). Thymic and splenic enlargement were evident by 4 weeks of age, but gross hyperplasia of the pituitary was not evident in p27$^{-/-}$ mice until 8–10 weeks of age.

The possibility of an endocrine contribution to the increased size of p27-deficient mice was evaluated by measuring serum levels of growth hormone (GH) and insulin-like growth factor 1 (IGF-1), the major hormonal

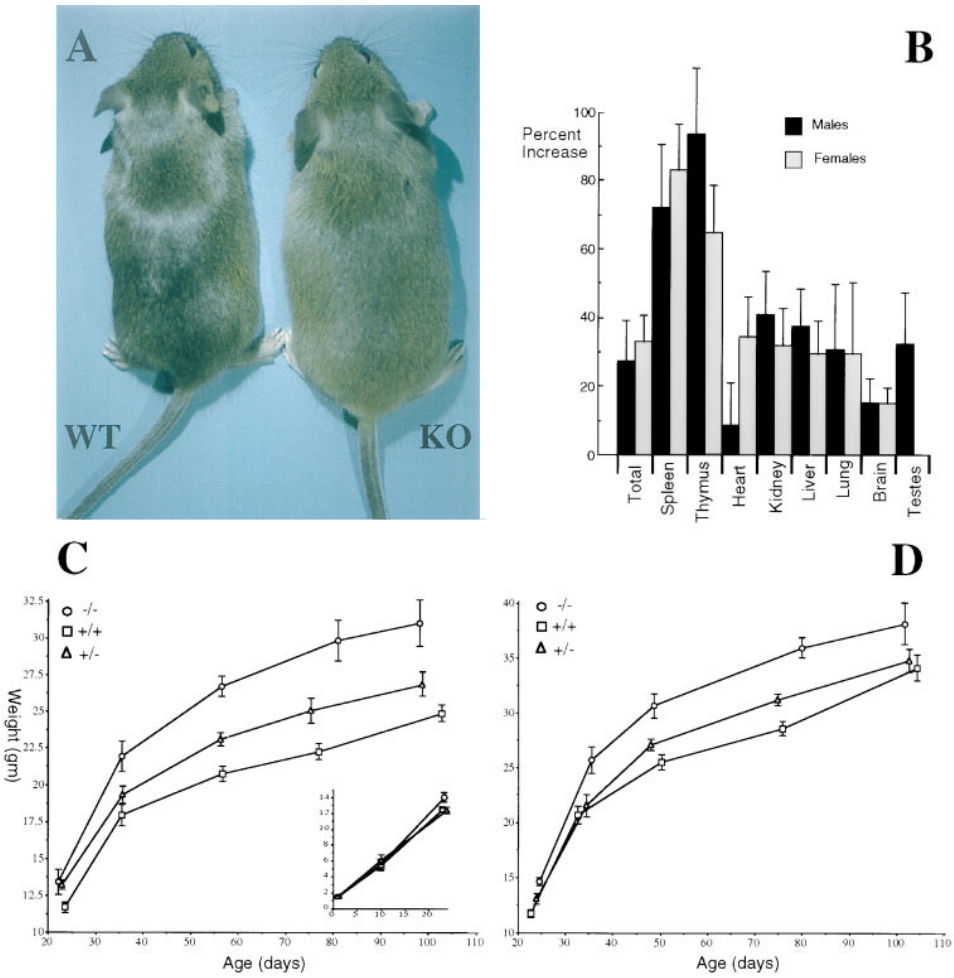


Figure 2. Increased Growth of p27-Deficient Mice

(A) Photograph of a $p27^{-/-}$ mouse and a control littermate at 6 weeks of age.

(B) Mean and 95% confidence interval of organ weights from 20 control and $p27^{-/-}$ mice at 6–7 weeks of age. Plotted is percent increase in weight in knockout mice compared with control mice.

(C) Mean and 95% confidence interval of weights of 30 control, $p27^{+/-}$, and $p27^{-/-}$ female mice as a function of age. Inset shows weights of a separate group of 20 male plus female mice weighed at birth and at 10 days. Data from 21 days is the mean of the results from the first group.

(D) Same as (C), but data were obtained from male mice.

determinants of postnatal growth. The mean serum levels of GH, IGF-1, and IGF-1-binding protein in four knockout males at either 6 or 12 weeks of age were not significantly different from levels in control littermates (data not shown).

### General Anatomic and Histologic Features

The in vivo distribution of p27 protein in mice ranging in ages from 4–18 weeks was evaluated by immunohistochemistry. Virtually all tissues in control mice expressed p27, its subcellular localization was almost exclusively nuclear, and immunoblots confirmed its ubiquitous pattern of expression (data not shown). As a general rule, p27 protein expression was restricted to nonproliferating cells. In the intestine, for example, p27-positive cells were localized to the quiescent cells occupying the mid and apical regions of the villi and were rare in the proliferating basal region (data not shown). Tissues from $p27^{-/-}$ mice did not exhibit specific immunostaining (data not shown; see Figure 7D).

The majority of tissues (listed in Experimental Procedures) obtained from 6-week-old $p27^{-/-}$ mice displayed normal histologic characteristics. No cellular hypertrophy was observed, in contrast with what has been reported in giant mice expressing a GH transgene. Only the pituitary and ovary were remarkable, and the histologic features of those organs are described in detail below. We also noted a subtle disorganization of the retina, characterized by loss of the normally sharp boundary between the inner and outer nuclear layers.

Hyperplasia may result in increased cell density (and therefore a decrease in average cell size) independent of overall organ size. Cell density determinations were obtained from both the liver and the brain by counting

Table 1. Hepatocyte and Neuronal Cell Counts

| | Wild-Type | $p27^{-/-}$ | Relative Increase (%) |
|---|---|---|---|
| Liver (n = 6) | 133 (16) | 163 (14) | 23 |
| Brain (n = 3) | | | |
| Cerebral cortex | 82 (2.1) | 108 (2.0) | 32 |
| Hippocampus | 111 (3.5) | 147 (2.1) | 32 |
| Habenular nucleus | 152 (2.1) | 198 (8.6) | 30 |

The number of hepatocyte and neuronal cells per unit volume counted in separate experiments. Group means (and standard deviations) represent the number (n) of animals indicated. The relative increase in hepatocyte and neuronal cell density in the $-/-$ mice was statistically significant ($p < 0.05$).

nuclei from fixed volume of tissue from anatomically identical regions. Hepatocyte cell density was increased an average of 23%, and neuronal cell density in each of three anatomically distinct forebrain regions was increased by approximately 30% in p27 knockout mice (Table 1). No other abnormalities in central nervous system neuroanatomy were found.

### Pituitary Adenomas

All p27 knockout mice over the age of 10 weeks (15 out of 15) developed 2- to 5-fold enlargement of the pituitary (Figures 3A and 3D). Histologic inspection revealed marked expansion of the pars intermedia (Figures 3B and 3E). This often caused compression and displacement of normal-appearing pars nervosa and pars distalis, but without direct invasion of the surrounding tissue. The cells had varying degrees of cytoplasmic basophilia and nuclear atypia. Interstitial hemorrhage was present in most specimens, resulting in lakes of fresh blood, hemosiderin deposits, and the brown pigmentation noted in gross specimens. Even in younger mice, no areas of normal pars intermedia surrounded the abnormal tissue, suggesting a progressive nonfocal process. Together these features indicate an adenomatous, neoplastic transformation of the pars intermedia cells. At 9 months of age, there has been no indication of early mortality in the 129/Sv × C57/B6J hybrids, but the majority of inbred (129/Sv) animals have died with massively enlarged pituitary tumors.

Transmission electron microscopy and immunocytochemistry together confirmed that the adenomatous cells arose from the pars intermedia. Electron microscopy revealed normal cytoarchitectural features of the pars nervosa and pars distalis in knockout mice. The cells comprising the abnormal tissue in knockout mice most closely resembled pars intermedia from normal mice (Figure 4). No ultrastructural features characteristic of normal pars distalis cells were present in the tumor tissue. Both control and knockout cells shared the same uniformly oval cytoplasm filled with low to moderately electron dense secretory vesicles and mitochondria, all characteristics of pars intermedia cells. However, the nuclei of knockout cells possessed more condensed chromatin and had a more bizarre configuration than control cells. The abnormal tissue stained positively for α melanocyte-stimulating hormone, β-endorphin, and adrenocorticotropic hormone (Figure 3), a triad of proteins derived from the proopiomelanocortin (POMC) gene product and produced in pars intermedia. Using antibodies to the anterior pituitary hormones thyroid-stimulating hormone, follicle-stimulating hormone (FSH), luteinizing hormone (LH), prolactin, and GH, identical patterns of histochemical staining were found in the pars distalis of the control and knockout mice. None of

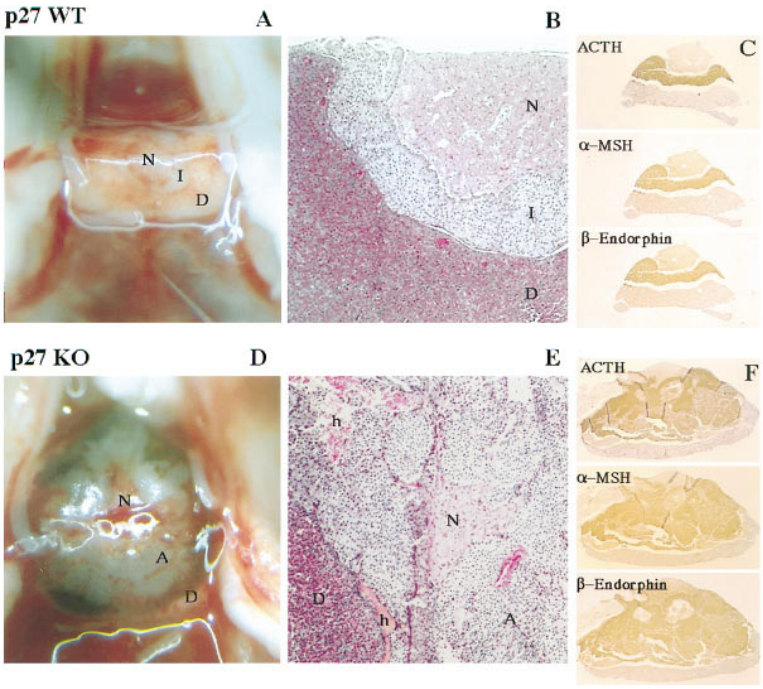


Figure 3. Pituitary Tumorigenesis in $p27^{-/-}$ Mice

(A and D) Dorsal views of pituitaries of 10-week-old control (A) and $p27^{-/-}$ mice (D) photographed in situ. The p27 null mouse pituitary is enlarged and hyperpigmented.

(B and E) Sections of pituitary stained with hematoxylin and eosin from control (B) and $p27^{-/-}$ mice (E) at 10 weeks of age (magnification, 40×). Indicated are the pars distalis (D), pars intermedia (I), and pars nervosa (N). The residual pars distalis and pars nervosa in the $p27^{-/-}$ pituitary are also indicated, as are the adenomatous cells of the abnormal pars intermedia (A) and areas of hemorrhage (h).

(C and F) Histologic sections of control (C) and $p27^{-/-}$ (F) pituitaries immunostained to detect expression of the indicated proteins (magnification, 10×).

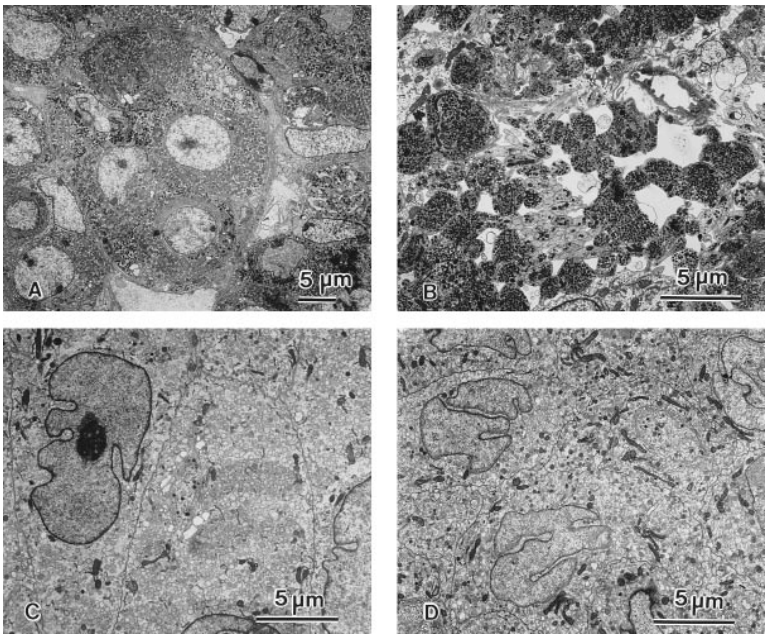


Figure 4. Ultrastructural Analysis of Tumor Cells Identifies Their Origin as the Pituitary Pars Intermedia

Transmission electron micrographs of pituitary pars distalis (A) (magnification, 1100×), pars nervosa (B), and pars intermedia (C) from $p27^{+/+}$ mice and the adenomatous tissue from a $p27^{-/-}$ littermate (D). (B)–(D) are viewed at 2000× magnification.

these hormones was expressed in cells of the adenomatous tumor tissue (data not shown).

**Lymphoid Populations**

While the disproportionate increase in pituitary size seen in $p27^{-/-}$ animals results from progressive neoplastic growth, thymic and splenic hyperplasia in these animals was not accompanied by notable histologic abnormalities (Figures 5A and 5B). Figure 5 graphically documents the dramatic increase in thymic cellularity in $p27^{-/-}$ mice, the thymi of which can contain more than $10^9$ cells. Despite this approximately 3-fold increase in the number of thymocytes, the development of these cells was remarkably unperturbed. Flow cytometric evaluation re-

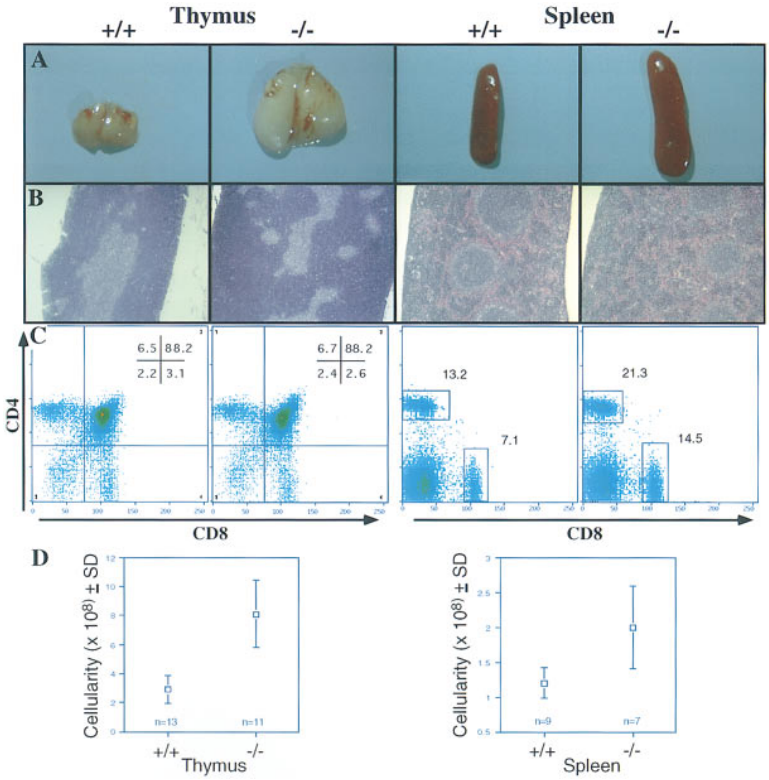


Figure 5. Thymic and Splenic Development in Control and $p27^{-/-}$ Mice

(A) Photographs of thymus and spleen from control and p27 null mice.

(B) Photomicrographs of control and $p27^{-/-}$ thymus stained with hematoxylin and eosin (magnification, 15×).

(C) Relative distribution of thymocyte subsets in the 6-week thymus were determined by staining for expression of the indicated lineage-specific cell surface antigens and sorting cells by flow cytometry. Relative percentages of cells with each cell surface characteristic are indicated.

(D) Absolute cell numbers (mean and standard deviation) in control and $p27^{-/-}$ thymus and spleen.

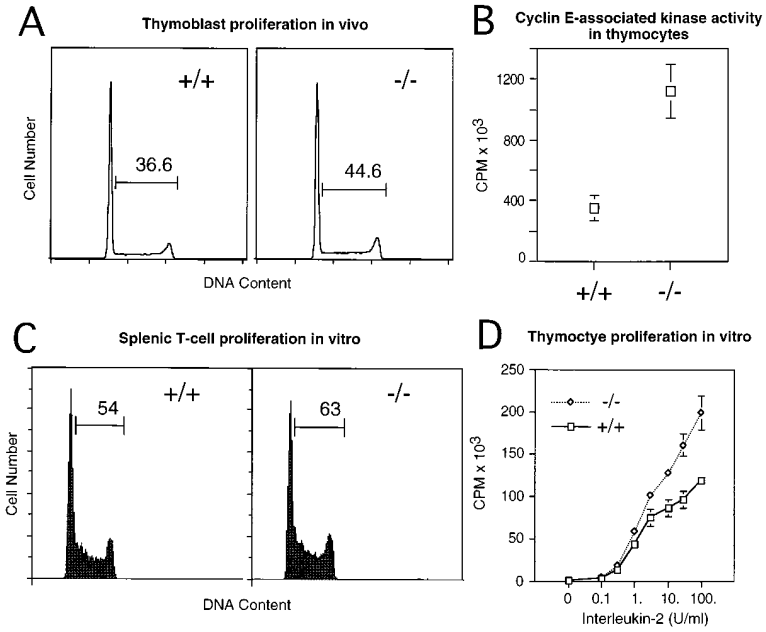


Figure 6. Increased Proliferation of p27$^{-/-}$ T Lymphocytes In Vivo and In Vitro

(A) Increased S phase fraction of p27$^{-/-}$ thymoblasts. Representative histograms from one wild-type and one p27$^{-/-}$ animal are shown. Similar results were obtained for fractionated CD4$^+$, CD8$^+$, or CD4$^+$CD8$^+$ blast subpopulations.

(B) Increased cyclin E–associated histone H1 kinase activity in p27$^{-/-}$ thymocytes. Results were quantitated by phosphorimaging, and mean and standard deviation values from 6 controls and 12 p27$^{-/-}$ samples are shown.

(C) Enhanced mitogenic activation of p27$^{-/-}$ splenic T cells in vitro. Splenic T cells were stimulated for 48 hr in vitro using plate-bound anti-CD3 antibodies and IL-2. DNA content was determined by flow cytometry, and percent values for S/G2/M phase cells are shown.

(D) Enhanced mitogenic activation of p27$^{-/-}$ thymocytes in vitro. Whole thymocyte preparations were stimulated using anti-CD3 antibodies and a titration of IL-2 for 48 hr, pulsed with [$^3$H]thymidine, and harvested 15 hr later (Appleby et al., 1992). Data shown are means and standard deviations (for controls) or standard errors (for p27$^{-/-}$) derived from two wild-type and four p27$^{-/-}$ mice.

vealed normal proportions of immature CD4$^-$8$^-$ thymocytes, a population that ordinarily includes the highest percentage of replicating cells, and of their more mature CD4$^+$8$^+$ progeny (Figure 5A). Moreover, the selective processes that permit emergence of mature, single-positive (CD4$^+$8$^-$ and CD4$^-$8$^+$) thymocytes, and their export to peripheral lymphoid organs, appeared grossly intact (Figure 5; data not shown). Hence, the absence of p27 results in impressive thymic hyperplasia without imposition of appreciable developmental pathology.

Splenocytes of p27$^{-/-}$ mice were also more abundant than in control mice (Figure 5B), resulting in part from the increased representation of T lymphocytes (Figure 5B). Indeed, the absolute number of B lymphocytes in the spleens of these animals, defined as B220$^+$, surface immunoglobulin–bearing cells, was normal (data not shown). In addition, a population of large, heterogeneous, CD3$^-$, B220$^-$, GR-1$^-$, Mac-1$^-$ cells was variably increased in abundance in the p27$^{-/-}$ spleens (data not shown). These cells almost certainly include immature hematopoietic progenitors (see below).

A direct effect of p27 deficiency on cell proliferation could be demonstrated in thymic and splenic T cells. p27$^{-/-}$ thymoblasts harvested directly from the animal had an increased percentage of S phase cells and a 3- to 4-fold increase in cyclin E–associated kinase activity when compared with control thymocytes (Figures 6A and 6B). A similar increase in cyclin E–associated kinase activity was observed in purified splenic T cells (data not shown). Increased mitogen responsiveness of p27$^{-/-}$ splenic and thymic T cells was also seen in vitro (Figures 6C and 6D). These results are consistent with previous experiments implicating p27 in modulating the mitogenic effect of interleukin-2 (IL-2) (Firpo et al., 1994; Nourse et al., 1994). TUNEL assays indicated that the percentage of apoptotic cells was the same in control and p27$^{-/-}$ thymocytes (data not shown). Together, these data suggest that the increased numbers of thymocytes in p27$^{-/-}$ mice was due to increased cell proliferation rather than diminished cell death.

### Hematopoietic Progenitors

Peripheral blood cell counts of erythrocytes, neutrophils, monocytes, and platelets were normal in the p27$^{-/-}$

Table 2. Hematopoietic Colony Formation

| | GFU-GM | CFU-E | CFU-MK | BFU-E |
|---|---|---|---|---|
| Femur | | | | |
| Wild type | 25.5 ± 1.2 | 88.0 ± 14.7 | 4.42 ± 0.73 | 2.60 ± 143 |
| p27 null | 34.2 ± 1.4 | 120.0 ± 22.7 | 4.10 ± 0.55 | 4.61 ± 0.94 |
| p[a] | 0.02 | 0.20 | 0.50 | 0.10 |
| Spleen | | | | |
| Wild type | 2.90 ± 0.61 | 135 ± 16.3 | 2.58 ± 0.24 | 1.03 ± 0.34 |
| p27 null | 9.34 ± 0.54 | 440 ± 144 | 7.37 ± 0.86 | 3.11 ± 0.36 |
| p[a] | 0.001 | 0.05 | 0.05 | 0.15 |

Shown are total numbers of colony-forming units ($\times 10^3$) per organ.
[a]Statistics by Mann–Whitney test.

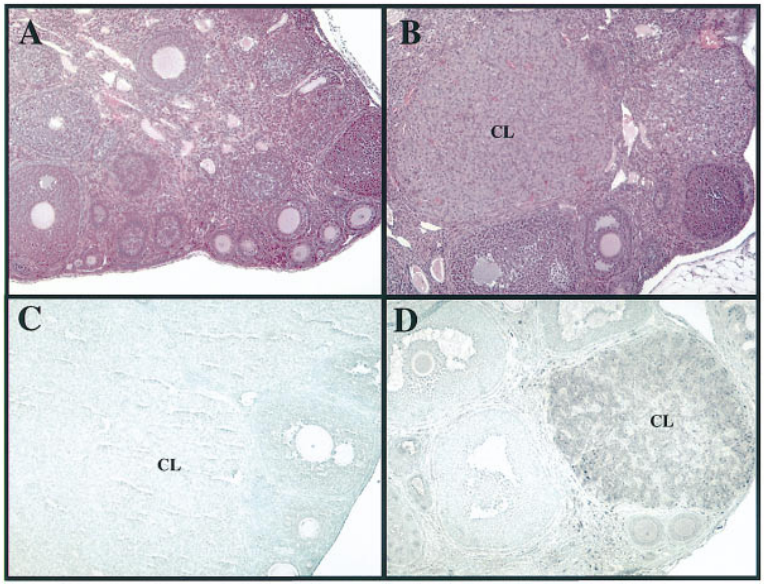


Figure 7. Luteal Phase Defect in the $p27^{-/-}$ Ovary

Sections of 10-week-old p27 null ovaries stained with hematoxylin and eosin (A) (magnification 25×) lack corpora lutea (CL), which are normally found in the control (B). Corpora lutea appear in $p27^{-/-}$ ovaries (C) following gonadotropin administration. Corpora lutea in control ovaries stain intensely for p27 protein expression (D) ([C] and [D] represent immunoperoxidase detection of p27 protein with methyl green counterstain).

mice compared with age-matched controls. However, we noted significant increases in the numbers of multiple types of hematopoietic progenitors. In four separate experiments, the number of granulocyte-macrophage (CFU-GM), early and late erythroid progenitors (BFU-E and CFU-E), and megakaryotic progenitors (CFU-MK) increased in both the marrow and spleen. The increase in progenitor levels was more pronounced in the spleen than the marrow. In the spleen, the increase in CFU-GM ranged from 3.2- to 9.4-fold, reaching statistical significance in each of four experiments and in the aggregate ($p < .004$). The number of marrow CFU-GM increased from 1.3- to 2.0-fold, statistically significant in the aggregate ($p < .004$). A representative experiment using inbred animals is shown (Table 2). These hematopoietic progenitor cell increases are consistent with the increase in splenic cellularity and suggest that the effect of p27 is exerted at an early stage of cell lineage determination.

### Female Sterility

Male $p27^{-/-}$ mice sired normal-sized litters, but female $p27^{-/-}$ mice did not become pregnant, even when paired with control males. The histologic appearance of the uterus and ovary at ages 3, 6, and 10 weeks of age was normal except for the conspicuous absence of corpora lutea in mature knockout females (Figures 7A and 7B). Of six knockout breeder pairs checked daily for 1 month, only two spontaneous copulation plugs were found. Oocytes were isolated from the oviduct of one of these females on gestation day 0.5, demonstrating that the block to ovulation was not fully penetrant. The luteal phase defect in $p27^{-/-}$ females did not appear to be due to lack of circulating gonadotropins or the inability to produce peak levels of these hormones, because average levels of FSH and LH were comparable in knockouts at both baseline and post-oopherectomy (data not shown). However, administration of super-physiologic levels of gonadotropins (superovulation) consistently induced ovulation, as evidenced by the presence of histologically normal corpora lutea (Figure 7C) and the ability to recover of oocytes at 0.5 days postcoitum (dpc). Together this implies that loss of p27 causes a relative resistance of the ovary to luteinizing hormones. p27 is highly expressed in the cells of control corpora lutea, consistent with a possible role for p27 in granulosa cell luteal differentiation (Figure 7D). Progesterone rose appropriately starting at day 4.5 in knockouts following superovulation, demonstrating at least partial function of the artificially induced corpora lutea (data not shown).

Superovulation produced numerous (5–20) preimplantation embryos at day 3.5 in each of four $p27^{-/-}$ females paired with knockout males. In fact, transfer of these preimplantation embryos to the uterus of pseudopregnant control recipients produced normal-sized litters, excluding the possibility that sterility is due to loss of a circulating fetal factor (e.g., chorionic gonadotropin). Superovulation was not sufficient to induce successful pregnancies in any of a dozen plugged knockout females (but was successful in three of four controls). Despite superovulation, gross and histologic inspection of the uterus showed that no implantation occurred in the majority of knockout mice. Among three mice that showed evidence of uterine implantation, the number of sites of implantation was greatly reduced, but appeared histologically normal; both a uterine decidual reaction and postimplantation embryos were present. The uterine environment in p27 null females was inadequate, since neither successful ovulation nor implantation was sufficient to produce a successful pregnancy.

## Discussion

### Increased Growth of p27-Deficient Mice

$p27^{Kip1}$ gene dosage determined animal size; $p27^{+/-}$ hemizygotes were intermediate in size between the small $p27^{+/+}$ and large $p27^{-/-}$ homozygotes. Although the p27-deficient animals were considerably heavier than controls, they were not obese. Essentially all organs in a p27 nullizygous mouse were at least 20% larger than controls. This was caused by increase in cell number,

rather than an increase in cell size or the amount of extracellular material.

Increased animal size can be associated with endocrine abnormalities. Gigantism results from the enforced overexpression of either GH (Palmiter et al., 1982) or IGF-1 (Mathews et al., 1988). IGF-2 has also been implicated as a determinant of animal size, primarily during embryonic growth (DeChiara et al., 1990). The presence of pituitary pathology, and the concomitant defects in fertility, raised the question of whether hormonal changes might underlie the increased size of the p27 knockouts. However, the adenomatous cells of the pars intermedia did not express GH, nor were there increased numbers of GH-producing cells in the normal-appearing pars distalis. In addition, mice lacking p27 had normal serum levels of both GH and IGF-1, and serum levels of IGF-1-binding protein were within normal limits, arguing against a shift in the amount of bound versus free IGF-1. Nor did the pattern of accelerated growth parallel what has been described for mice overproducing GH, IGF-1, or IGF-2. GH and IGF-1 transgenic mice have normal birth weights; growth is not accelerated until after 3–4 weeks or 6–8 weeks of age, respectively. Mice systemically overproducing IGF-2 are born heavier than controls, but increased size is not maintained into adulthood (Wolf et al., 1994). In contrast, $p27^{-/-}$ mice are not larger than controls at birth, but attain an increased size within the first 3 weeks of life and are larger as adults. GH, IGF-1, and IGF-2 can cause organomegaly (Palmiter et al., 1983; Mathews et al., 1988; Quaife et al., 1989; Wolf et al., 1994; Ward et al., 1994; Buul-Offers et al., 1995). However, only selected organs are affected, and this contrasts with the generalized organomegaly in the $p27^{-/-}$ mouse. In sum, when the pattern and timing of organ enlargement, the histologic features of affected organs, and the apparently normal serum hormone levels are all taken into consideration, the overall picture is incompatible with previous descriptions of gigantism due to endocrine effects.

The effect of p27 on animal size may be cell autonomous, an idea most consistent with the molecular biology of p27 function (see Introduction). This would represent an example of a cell-autonomous determinant of size in multicellular organisms. The absence of p27 may allow continued cell proliferation despite low or absent mitogenic stimuli, the outcome being generalized hyperplasia and increased body size. Indeed, we have shown both increased proliferation in vivo and increased mitogen responsiveness in vitro of $p27^{-/-}$ thymic and splenic T lymphocytes. One extreme model, which we can exclude, is that loss of p27 caused massive increases in cell proliferation that were largely balanced by increased cell death. This conclusion is based on the fraction of S phase cells in various tissues measured by fluorescence-activated cell sorter (FACS) analysis and bromodeoxyuridine (BrdU) staining, combined with the absence of an increased number of apoptotic cells. It is more likely, therefore, that p27 deficiency increases cell proliferation to an extent that is concordant with the overall increase in cell number. The threshold that p27 imposes on CDK activation and cell proliferation apparently is regulated very tightly. Even a partial decrease in p27 levels appears to increase cell proliferation in vivo, as evidenced by the increased size of p27 hemizygotes.

Independent support for a cell cycle defect in p27-deficient cells emerged from our analysis of cell density in various tissues. In liver and brain, we showed that $p27^{-/-}$ cells were smaller than control cells. The smaller size of p27-deficient cells is similar to the effect caused by overexpressing G1 cyclins (Cross, 1988; Ohtsubo and Roberts, 1993; Quelle et al., 1993) and may reflect altered coupling between cell growth and the cell division cycle.

**Pituitary Tumorigenesis**

By histological, ultrastructural, and immunocytochemical criteria, adenomatous growth in the $p27^{-/-}$ mice was restricted to the melanotrophic cells of the pars intermedia. Pituitary pathology was grossly evident by 2–3 months of age, but histologic inspection of pituitaries from mice as young as 4–6 weeks showed uniform pars intermedia hyperplasia. In these young mice, there was no evidence of focal lesions surrounded by normal-appearing tissue. Thus, not only did the pituitary tumors occur with 100% penetrance, but they appeared to involve the entire pars intermedia. This suggested that loss of p27 was sufficient to cause abnormal proliferation and that occurrence of a second genetic event may not be required. By 9 months of age, p27 nullizygotes showed no significant occurrence of other tumors, and this is consistent with the absence of homozygous p27 mutations in primary human tumors (Pietenpol et al., 1995; Ponce-Castenada et al., 1995; Kawamata et al., 1995). However, the dosage effect of p27 gene deletions on mouse body size suggests that the hemizygous deletions of p27 found in human hematopoietic malignancies (Pietenpol et al., 1995; Sato et al., 1995) may enhance cell proliferation and contribute to malignant progression.

Pituitary tumors in both mice and humans usually arise as adenomas within the pars distalis, and tumors of the pars intermedia are rare. It is striking that deletions of p27 or *Rb* (retinoblastoma) (Williams et al., 1994; Hu et al., 1994) are the only gene defects known that cause pars intermedia tumors, and both do so with almost 100% penetrance. It is plausible, therefore, that the unusual pattern of tumor development shared by p27 and *Rb* mutant mice is a consequence of the interaction of these proteins in a common regulatory pathway. p27 inhibits kinase activity of CDK2–cyclin E/A, CDK4–cyclin D, and CDK6–cyclin D complexes. All these kinases phosphorylate the Rb protein in vitro, and correlations have been drawn between their activation and Rb phosphorylation in vivo. If p27 were the primary regulator of Rb phosphorylation in the pars intermedia, then the absence of p27 might allow constitutive hyperphosphorylation and inactivation of Rb and transformation of the pars intermedia melanotrophs.

Melanotroph proliferation may be primarily under negative control by the neurotransmitter dopamine. Dopaminergic innervation coincides with inhibition of melanotroph proliferation in developing rats, and pharmacologic agonists or antagonists of dopamine inhibit or promote melanotroph proliferation, respectively, both in vivo and in vitro (Gary and Chronwall, 1992; Gehlert et al., 1988; Chronwall et al., 1987). The anti-proliferative effect of dopamine may be exerted at a point in the cell

cycle where both p27 and Rb are required to maintain cell cycle arrest. Alternatively, the loss of p27 may impair the development or function of the dopaminergic neurons that innervate the pars intermedia. By either model, the unique behavior of these cells may be the consequence of the fact that their proliferation is primarily determined by removal of an inhibitory signal, whereas the proliferation of most other cell types is often dependent upon provision of a growth stimulus.

### Female Sterility

Deletion of p27 caused female specific sterility. Secondary ovarian follicles developed, but did not progress to form corpora lutea. Gonadotropin production did not appear to be impaired, because normal numbers of FSH- and LH-producing cells were visualized by immunohistochemical staining in the anterior pituitary and both basal and peak serum levels of FSH and LH were normal. One clue to the origin of the infertility may be that p27 protein was highly expressed in corpora lutea of control mice. Thus, p27 deficiency may impart a relative resistance to the action of LH on the mature follicle. In accord with this idea, exogenous administration of greater than physiological amounts of gonadotropins induced ovulation, differentiation of corpora lutea, and early development of viable embryos in knockout females. These embryos implanted but did not develop to term in the knockout females, raising the possibility that the absence of p27 caused a second block to development intrinsic to the uterus. In sum, p27-deficient mice have both ovarian and uterine dysfunction, but it is not yet known whether these are a direct effect of the absence of p27 in the reproductive organ.

### Progenitor Cell Hyperplasia

p27 is expressed at high levels in nondividing cells, including cells that have become quiescent in response to mitogen depletion and those that have become postmitotic as part of a program of terminal differentiation. The phenotype of the p27-deficient mice suggested that p27 is important for the former response but dispensable for the latter. This is best illustrated and was most carefully analyzed in the thymus, where dramatic hyperplasia had no detectable impact on thymic development or thymocyte differentiation. Each of the normal thymocyte subpopulations were increased in number and in the correct proportion to one another; there was no evidence for neoplastic growth or selective expansion of a subset of thymocytes. The spleen in the p27 nullizygous mouse was also disproportionately hyperplastic, yet its histologic organization appeared normal and cells from all hematopoietic lineages were normally represented. Histologic examination suggested that these conclusions applied without exception to other tissues as well. The vast majority of tissues in mice lacking $p27^{Kip1}$ had essentially no pathologic abnormalities, and the $p27^{+/-}$ hemizygotes, apart from their increased size, appeared totally normal.

In the thymus and spleen, we have shown that the loss of p27 leads to increased numbers of hematopoietic progenitor cells. It is difficult to measure accurately progenitor or stem cell numbers in other organs, but one idea is that p27 deficiency may induce hyperplasia of the committed progenitor or stem cells for many lineages and that this is the developmental basis for the increased overall size of the knockout mice. In fact, we have observed that the relative increase in hematopoietic progenitor cells in the spleen is greater than the relative increase in their differentiated descendants (e.g., more than a 3-fold increase in splenic CFU-E and CFU-GM, but less than a 2-fold increase in the numbers of mature cells in the spleen and peripheral blood; Table 2; data not shown). Thus, p27 may have a selective effect on the self-renewing, mitogen-driven cell cycles characteristic of stem and some progenitor cells. However, once cells embark on a program of differentiation, they often undergo a relatively fixed number of programmed cell divisions and enter a state of mitogen-independent cell cycle arrest. Since p27 appears to be primarily involved in the cellular response to extracellular mitogens, its absence might have relatively little impact during the process of terminal differentiation. In this regard, the disproportionate growth of the thymus compared with other tissues in the $p27^{-/-}$ mouse is interesting, especially in the light of evidence that p27 may have a key role during mitogenic activation of mature T lymphocytes by IL-2 (Firpo et al., 1994; Nourse et al., 1994). This points out that the distinction between mitogen-dependent proliferation of progenitor versus fully differentiated cells must be drawn carefully. p27 appears to play an ongoing role in some differentiated cells, such as T lymphocytes, which retain the ability to proliferate in response to mitogenic signals.

## Experimental Procedures

### Production of p27 Null Mice

A 17 kb NotI fragment containing the entire coding region of the p27 gene was obtained from a mouse 129/Sv λ genomic library (obtained from Paul Stein) using a p27 cDNA probe. pKNT was constructed by subcloning a 7 kb XhoI fragment and a 1.8 kb BglII–EcoRI genomic DNA fragment into the targeting vector pPNT (Tybulewicz et al., 1991). pKNT was linearized with HindIII and transduced by electroporation into mouse XY AK7 ES cells (courtesy of Phillipe Soriano; Soriano et al., 1991). ES cells were selected in 400 μg/ml G418 and 0.2 μM FIAU. Colonies of ES cells with homologous recombination events were identified by PCR amplification of a 2 kb fragment using a primer derived from p27 genomic DNA sequences downstream from exon 2 (K2, TTCTTACCGAAAGGGACACTAATC) and from the neomycin gene (N1, CCTTCTATGGCCTTCTTGACG). PCR reactions were performed for 40 cycles (93°C for 30 s; 55°C–57°C for 30 s; 65°C for 2 min) as previously described (Kogan et al., 1987). Southern blots using probes external to both the 5′ and 3′ end of the targeting construct confirmed that a homologous recombination occurred in each of the six clones used for blastocyst injection. $p27^{-/+}$ ES cells were introduced by microinjection into 5 dpc C57/B6J mouse embryos. Germline transmission was identified in male chimeras representing three separate ES cell clones. Homozygous p27 deletions in the F2 generation were confirmed by the presence of a 0.5 kb PCR fragment unique to the mutant transgene with primers N1 and K3 (TGGAACCCTGTGCCATCTCTAT) and the absence of the corresponding 0.9 kb fragment unique to the wild-type allele using primers K3 and K5 (GAGCAGACGCCCAAGAAGC).

### Anatomic and Histologic Assessment

A cohort 30–40 F2 generation hybrids from each genotype ($p27^{-/-}$, $p27^{-/+}$, and $p27^{+/+}$) was observed and weighed at regular intervals. We weighed 6- to 7-week-old mice (both congenic 129/Sv and hybrid C57/B6J) at necropsy to confirm the absolute differences in animal size. Internal organs were weighed, and the following tissues

were fixed in 10% neutral buffered formalin (Sigma): brain, pituitary, eye, lacrimal gland, trachea, esophagus, heart, lung, thymus, axillary lymph node, liver, stomach, duodenum, colon, kidney, adrenal, pancreas, urinary bladder, testis, ovary, uterus, skin, and femur. Tissues were paraffin embedded, cut in 5 μm sections and stained with hematoxylin and eosin. Brains and pituitaries were fixed in 4% paraformaldehyde for immunoperoxidase staining and cell counts by first perfusing the animal with PBS and then fixative. Hematopoietic differential cell counts were obtained from Wright–Giemsa-stained blood smears and cytospin preparations of marrow and spleen.

**Transmission Electron Microscopy**

We anesthetized 5-month-old male control and knockout mice, perfused them with 2% glutaraldehyde, 2% paraformaldehyde in 0.1 M phosphate buffer, and postfixed the pituitaries and brains in 2% glutaraldehyde, 2% paraformaldehyde in 0.1 M phosphate buffer for 4 hr. Tissue was washed three times overnight in 0.2 M cacodylate buffer, fixed in 2% $OsO_4$ for 1 hr, dehydrated in graded ethanol solutions, immersed in propylene oxide, and embedded in LX-12 (Ladd Industries). Parasagittal pituitary sections (60–90 nm) were cut, mounted onto grids, and counterstained with uranyl acetate and lead citrate. Grid-mounted sections were examined in a JEOL 1200 EX-1 microscope, and fields were photographed at magnifications ranging from 2000× to 4000× at 120 kV.

**Cell Counts from Brain and Liver**

Cell counts were obtained from hematoxylin–eosin-stained sections of forebrain from three wild-type and three knockout male mice. Neurons were counted at 400× magnification in the following anatomic loci: 1 cm diameter column of full-thickness cerebral cortex located at the junction of anterior corpus callosum and cingulum at the level of the adjacent habenular nucleus; the habenular nucleus; the rostral zone of dentate in hippocampus. Neurons were counted from identically circumscribed volumes on the basis of characteristic morphology found on hematoxylin–eosin stain. The average of three separate counts was obtained from each site in each mouse. Counts from both 3-month-old and 5-month-old mice were combined for analysis, since neurons are already postmitotic at birth and their cerebral number is fixed. Separate groups of six $p27^{-/-}$ and six sex-matched controls were used to measure the density of hepatocytes in 0.4 μm hematoxylin–eosin-stained tissue sections from the areas surrounding single hepatic venules. Polaroid photographs were obtained, and the number of hepatocyte nuclei in 12 high power fields from each animal was counted.

**Antibodies**

Affinity-purified rabbit anti–mouse p27 antibody was courteously provided by R. Sheaff. Anti-β-FSH and anti-GH antibodies were obtained from the National Pituitary Agency. Anti-β-LH was a gift of L. Duhamel. Both anti-prolactin and anti–thyroid-stimulating hormone antibodies were obtained from INCSTAR. Anti–adrenocorticotropic hormone, anti–α melanocyte-stimulating hormone, and anti-β-endorphin antibodies were obtained from BioGenex Labs.

**Immunoperoxidase Staining**

Tissues were stained for the presence of p27 using biotinylated secondary antibodies, followed by avidin–horseradish peroxidase plus DAB as a chromogen (Hsu and Soban, 1982). Pituitary sections were stained in a similar fashion for the presence of the pituitary hormones. Deparaffinized sections were blocked for endogenous peroxidase in 3% $H_2O_2$ for 5 min (for p27) or 30 min (for pituitary hormones). Specimens to be stained for the presence of p27 were microwaved for 10 min in the presence of citrate buffer (Gerdes et al., 1992; Hsu et al., 1981). Primary antibodies were applied for 60–90 min (p27, 1:100; β-FSH, 1:1000; GH, 1:2000; β-thyroid-stimulating hormone, 1:1000; β-LH, 1:1000; prolactin, 1:3000). In each case, negative controls did not include primary antibody, and positive controls were identically treated specimens from control mice.

**Flow Cytometric Analysis**

Single cell suspensions of thymocytes and splenocytes were prepared as described previously (Cooke et al., 1991). Cells were stained for surface expression of CD4 and CD8 using fluorescein isothiocyanate–labeled Lyt-2 (clone CT-CD4) and phycoerythrin-conjugated L3T4 (clone CT-CD8a) (Caltag Laboratories), respectively. Events were collected in list mode files on a FACS-Star flow cytometer (Beckton Dickinson) and analyzed using Repro-Mac software (True Facts Software).

**Hematopoietic Progenitor Assays**

Femurs, tibiae, and spleens were removed aseptically, marrow cells were flushed into Iscove's modified medium (IMDM) containing 10% fetal calf serum and single cell suspensions made by aspirating cells through smaller-gauge needles. Colony-forming assays were performed in triplicate as described previously (Broudy et al., 1995). In brief, for CFU-GM and CFU-MK determinations, $1 \times 10^5$ marrow or $1 \times 10^6$ spleen cells were plated in a 1 ml culture plate in IMDM containing 15% horse serum, 100 U/ml murine IL-3, 30 ng/ml human IL-11, 1000 U/ml murine TPO, 1% penicillin–streptomycin–fungizone, $5 \times 10^{-5}$ M β-mercaptoethanol, 2 U/ml human erythropoietin, 1.5% pokeweed mitogen-stimulated murine spleen cell–conditioned medium and were made semisolid with 0.28% agar. Cultures were incubated for 5 days in a humidified atmosphere containing 5% $CO_2$. Early erythroid progenitors (BFU-E) were cultured, as described, in IMDM supplemented with 30% fetal calf serum, 1% BSA, $5 \times 10^{-5}$ β-mercaptoethanol and made semisolid with 1.4% methylcellulose (Kaushansky et al., 1994). Late erythroid progenitors (CFU-E) were quantified in a plasma clot assay as previously described (Broudy et al., 1988). Megakaryocyte colonies containing more than three large refractive cells and myeloid and erythroid colonies containing more than 40 cells were enumerated by inverted electron microscopy.

**Fertility and Endocrine Investigations**

Breeding capacity was determined with four to six pairs of breeders of every genetic combination (−/−, +/−, and +/+). Results were confirmed in congenic (129/Sv) mice. Superovulation of 5-week-old F2 generation hybrid females was performed as described by administering pregnant mare's serum (5 U intraperitoneally; Sigma), followed by hCG (5 U intraperitoneally) 48 hr later (−0.5 dpc). Peptide hormone assays were performed by $^{125}$I-RIA using known concentrations of hormone for standard curves. Retro-orbital blood was obtained under moderate anesthesia provided by halothane inhalation in four $p27^{-/-}$ and four age- and sex-matched controls. GH levels were determined by RIA (Amersham) in both 6- and 12-week-old females (four knockout mice and four controls at each age). Likewise, serum was obtained for the following assays: IGF-1 and IGF-1-binding ligand, 4-month-old males; FSH and LH, 6- to 8-week-old females and 12-week-old females 2 weeks post-oopherectomy.

**Acknowledgments**

We thank Mark Gurian-West, Norma Fox, Nancy Lin, Laura Gatti, Kelly Wirtala for assistance with PCR, hematopoietic cultures, and histology. Phillipe Soriano and Paul Stein provided advice and assistance in the targeted disruption of the p27 gene in ES cells. Joe D'Ercole, William Bremner, and Nira Ben-Jonathan assayed IGF-1, FSH and LH, and prolactin levels, respectively. L. Duhamel, A. F. Parlow, and the National Pituitary Agency provided pituitary antibodies. We also thank Norm Wolf, Mark Groudine, Richard Palmiter, and colleagues at the Fred Hutchinson Cancer Research Center for suggestions during the course of this work and Andy Koff for discussing results prior to publication. Support for this work was provided by National Institutes of Health (NIH) grants R01 CA 31615 and R01 DK 49855 to K. K., NIH grant GM53049 to L. -H. T., NIH grant KO8 NSO1661-01A1 to M. R., National Cancer Institute (NCI) grant CA45682 and the Poncin Scholarship Fund to R. M. P. and M. T., pilot project funds from the NCI (R21 CA66186) to P. P., and a Susan Komen fellowship to E. F.; J. M. R., E. F., and M. L. F. were supported by grants from the NIH and the Fred Hutchinson Cancer Research Center.

Received March 8, 1996; revised April 19, 1996.

**References**

Appleby, M.W., Gross J.A., Cooke, M.P., Levin, S.D., Qian X., and Perlmutter, R.M. (1992). Defective T cell receptor signaling in mice lacking the thymic isoform of p59$^{fyn}$. Cell *70*, 751–763.

Broudy, V.C., Tait, J.F., and Powell, J.S. (1988). Recombinant human erythropoietin: purification and analysis of carbohydrate linkage. Arch. Biochem. Biophys. *265*, 329–336.

Broudy, V.C., Lin, N.L., and Kaushansky, K. (1995). Thrombopoietin (c-mpl ligand) acts synergistically with erythropoietin, stem cell factor, and interleukin-11 to enhance murine megakaryocyte colony growth and increases megakaryocyte ploidy *in vitro*. Blood *85*, 1719–1726.

Brugarolas, J., Chandrasekaran, C., Gordon, J., Beach, D., Jacks, T., and Hannon, G. (1995). Radiation-induced cell cycle arrest compromised by p21 deficiency. Nature *377*, 552–557.

Chronwall, B., Millington, W., Griffin, W., Unnerstall, J., and O'Donohue, T. (1987). Histological evaluation of the dopaminergic regulation of proopiomolanocortin gene expression in the intermediate lobe of the rat pituitary, involving *in situ* hybridization and [$^3$H]thymidine uptake measurement. Endocrinology *12*, 1201–1211.

Coats, S., Flannagan, W.M., Nourse, J., and Roberts, J. (1996). Requirement of p27$^{Kip1}$ for restriction point control of the fibroblast cell cycle. Science, in press.

Cooke, M.P., Abraham, K.M., Forbush, K.A., and Perlmutter, R.M. (1991). Regulation of T cell receptor signaling by a src family protein-tyrosine kinase (p59fyn). Cell *65*, 281–291.

Cross, F. (1988). DAF1, a mutant gene affecting size control, pheromone arrest, and cell cycle kinetics of *Saccharomyces cerevisiae*. Mol. Cell. Biol. *8*, 4675–4684.

DeChiara, T., Efstratiadis, A., and Robertson, E. (1990). A growth deficiency phenotype in heterozygous mice carrying an insulin-like growth factor II gene disrupted by targeting. Nature *345*, 78–80.

Deng, C., Zhang, P., Harper, J.W., Elledge, S., and Leder, P. (1995). Mice lacking p2$^{CIP1/WAF1}$ undergo normal development but are defective in G1 checkpoint control. Cell *82*, 675–684.

El-Diery, W., Tokino, T., Velculescu, V., Levy, D., Parsons, R., Trent, J., Lin, D., Mercer, E., Kinzler, K., and Vogelstein, B. (1993). *WAF1*, a potential mediator of p53 tumor suppression. Cell *75*, 817–825.

Firpo, E., Koff, A., Solomon, M., and Roberts, J. (1994). Inactivation of a Cdk2 inhibitor during IL-2 induced proliferation of human T-lymphocytes. Mol. Cell. Biol. *14*, 4889–4901.

Flores-Rozas, H., Kelman, Z., Dean, F., Pan, Z., Harper, J.W., Elledge, S., O'Donnell, M., and Hurwitz, J. (1994). CDK-interacting protein 1 directly binds with proliferating cell nuclear antigen and inhibits DNA relication catalyzed by the DNA polymerase and holoenzyme. Proc. Natl. Acad. Sci. USA *91*, 8655–8659.

Gary, K., and Chronwall, B. (1992). The onset of dopaminergic innervation during ontogeny decreases melanotrope proliferation in the intermediate lobe of the rat pituitary. Int. J. Dev. Neurosci. *10*, 131–142.

Gehlert, D., Bishop, J., Schafer, M., and Chronwall, B. (1988). Rat intermediate lobe in culture: dopaminergic regulation of POMC biosynthesis and cell proliferation. Peptides *9* (Suppl. 1), 161–168.

Gerdes, J., Becker, M., and Key, G. (1992). Immunohistological detection of tumour growth fraction (Ki-67 antigen) in formalin-fixed and routinely processed tissues. J. Pathol. *168*, 85–86.

Gu, Y., Turek, C., and Morgan, D. (1993). Inhibition of CDK2 activity *in vivo* by an associated 20K regulatory subunit. Nature *366*, 707–710.

Halevy, O., Novitch, B., Spicer, D., Skapek, S., Rhee, J., Hannon, G., Beach, D., and Lasser, A. (1995). Correlation of terminal cell cycle arrest of skeletal muscle with induction of p21 by MyoD. Science *267*, 1018–1021.

Harper, J.W., Adami, G., Wei, N., Keyomarse, K., and Elledge, S. (1993). The p21 cdk-interacting protein Cip1 is a potent inhibitor of G1 cyclin-dependent kinases. Cell *75*, 805–816.

Hsu, S., and Soban, E. (1982). Color modification of diaminobenzidine (DAB) precipitation by metallic ions and its application for double immunohistochemistry. J. Histochem. Cytochem. *30*, 1079–1082.

Hsu, S., Raine, L., and Fanger, H. (1981). Use of biotin-avidin-peroxidase conplex (ABC) in immunoperoxidase techniques: a comparison between ABC and unlabeled antibody techniques. Am. J. Clin. Pathol. *75*, 816–821.

Hu, N., Gutsmann, A., Herbert, D.C., Bradley, A., Lee, W.H., and Lee, E.Y. (1994). Heterozygous Rb-1 $\delta$ 20/+ mice are predisposed to tumors of the pituitary gland with a nearly complete penetrance. Oncogene *9*, 1021–1027.

Kato, J., Matsuoka, M., Polyak, K., Massague, M., and Sherr, C. (1994). Cyclic AMP–induced G1 phase arrest mediated by an inhibitor (p27$^{Kip1}$) of cyclin-dependent kinase 4 activation. Cell *79*, 487–496.

Kaushansky, K., Lok, S., Holly, R.D., Broudy, V.C., Lin, N., Bailey, M.C., Forstrom, J.W., Buddle, M.M., Oort, P.J., Hagen, F.S., et al. (1994). Promotion of megakaryocyte progenitor expansion and differentiation by the c-Mpl ligand thrombopoietin. Nature *369*, 568–571.

Kawamata, N., Morosetti, R., Miller, S., Park, D., Spirin, K., Nakamaki, T., Takeuchi, S., Hatta, Y., Simpson, J., Wilcyznski, S., et al. (1995). Molecular analysis of the cyclin dependent kinase inhibitor gene p27/Kip1 in human malignancies. Cancer Res. *55*, 2266–2269.

Koff, A., Ohtsuki, M., Polyak, K., Roberts, J., and Massague, J. (1993). Negative regulation of G1 in mammalian cells: inhibition of cyclin E-dependent kinase by TGF-$\beta$. Science *260*, 536–539.

Kogan, S.C., Doherty, M., and Gitschier, J. (1987). An improved method for prenatal diagnosis of genetic diseases by analysis of amplified DNA sequences. N. Engl. J. Med. *317*, 985–990.

Lee, M., Reynisdottir, I., and Massague, J. (1995). Cloning of p57$^{Kip2}$, a cyclin-dependent kinase inhibitor with unique domain structure and tissue distribution. Genes Dev. *9*, 639–649.

Luo, Y., Hurwitz, J., and Massague, J. (1995). Cell-cycle inhibition by independent CDK and PCNA binding domains in p21 Cip1. Nature *375*, 159–161.

Mathews, L., Hammer, R., Behringer, R., D'Ercole, A.J., Bell, G., Brinster, R., and Palmiter, R. (1988). Growth enhancement of transgenic mice expressing human insulin-like growth factor I. Endocrinology *123*, 2827–2833.

Matsuoka, S., Edwards, M., Bai, C., Parker, S., Zhang, P., Baldini, A., Harper, J.W., and Elledge, S. (1995). p57$^{Kip2}$, a structurally distinct member of the p21$^{Cip1}$ cdk inhibitor family is a candidate tumor suppressor gene. Genes Dev. *9*, 650–662.

Noda, A., Ning, Y., Venable, S., Pereira-Smith, O., and Smith, J. (1994). Cloning of senescent cell-derived inhibitors of DNA synthesis using an expression screen. Exp. Cell Res. *211*, 90–98.

Nourse, J., Firpo, E., Flanagan, M., Meyerson, M., Polyak, K., Lee, M.-H., Massague, J., Crabtree, G., and Roberts, J. (1994). IL-2 mediated elimination of the p27$^{Kip1}$ cyclin-Cdk kinase inhibitor prevented by rapamycin. Nature *372*, 570–573.

Ohtsubo, M., and Roberts, J. (1993). Cyclin dependent regulation of G1 in mammalian fibroblasts. Science *259*, 1908.

Palmiter, R., Brinster, R., Hammer, R., Trumbauer, M., Rosenfeld, M., Birnberg, N., and Evans, R. (1982). Dramatic growth of mice that develop from eggs microinjected with metallothionein-growth hormone fusion genes. Nature *300*, 611–615.

Palmiter, R., Nordstedt, G., Gelinas, R., Hammer, R., and Brinster, R. (1983). Metallothionein-human growth hormone fusion genes stimulate growth of mice. Science *222*, 809–814.

Parker, S., Eichele, G., Zhang, P., Rawls, A., Sands, A., Bradley, A., Olson, E., Harper, J.W., and Elledge, S. (1995). p53-independent expression of p21$^{Cip1}$ in muscle and other terminally differentiating cells. Science *267*, 1024–1027.

Pietenpol, J., Bohlander, S., Sato, Y., Papadoupolos, B., Liu, C., Friedman, B., Trask, B., Roberts, J., Kinzler, K., Rowley, J., and Vogelstein, B. (1995). Assignment of the human p27$^{Kip1}$ gene to 12p13 and its analysis in leukemias. Cancer Res. *55*, 1206–1210.

Polyak, K., Kato, J.-Y., Solomon, M.J., Sherr, C.J., Massague, J.,

Roberts, J.M., and Koff, A. (1994a). $p27^{Kip1}$, a cyclin-Cdk inhibitor, links transforming growth factor-β and contact inhibition to cell cycle arrest. Genes Dev. *8*, 9–22.

Polyak, K., Lee, M.-H., Erdjument-Bromage, H., Koff, A., Roberts, J., Tempst, P., and Massague, J. (1994b). Cloning of $p27^{Kip1}$, a cyclin-dependent kinase inhibitor and a potential mediator of extracellular antimitogenic signals. Cell *78*, 59–66.

Ponce-Castenada, M., Lee, M., Latres, E., Polyak, K., Lacombe, L., Montgomery, K., Mathew, S., Krauter, K., Sheinfeld, J., Massague, J., et al. (1995). $p27^{Kip1}$: chromosomal mapping to 12p12–12p13.1 and absence of mutations in human tumors. Cancer Res. *55*, 1211–1214.

Quaife, C., Mathews, L., Pinkert, C., Hanner, R., Brinster, R., and Palmiter, R. (1989). Histopathology associated with elevated levels of growth hormone and insulin-like growth factor I in transgenic mice. Endocrinology *124*, 40–48.

Quelle, D., Ashmun, R., Shurtleff, S., Kato, J.Y., Bar-Sagi, D., Roussel, M., and Sherr, C.J. (1993). Overexpression of mouse D-type cyclins accelerates G1 phase in rodent fibroblasts. Genes Dev. *7*, 1559–1571.

Reynisdottir, I., Polyak, K., Iavarone, A., and Massague, J. (1995). Kip/Cip and Ink4 Cdk inhibitors cooperate to induce cell cycle arrest in response to TGF-β. Genes Dev. *9*, 1831–1845

Roberts, J.M., Koff, A., Polyak, K., Firpo, E., Collins, S., Ohtsubo, M., and Massague, J. (1994). Cyclins, Cdks, and cyclin kinase inhibitors. Cold Spring Harbor Symp. Quant. Biol. *59*, 31–38.

Sato, Y., Suto, Y., Pietenpol, J., Golub, T., Gilliland, G., Davis, E., Le Beau, M., Roberts, J., Vogelstein, B., Rowley, J., and Bohlander, S. (1995). TEL and KIP1 define the smallest region of deletions on 12p13 in hematopoietic malignancies. Blood *86*, 1525–1533.

Serrano, M., Hannon, G., and Beach, D. (1993). A new regulatory motif in cell-cycle control causing specific inhibition of cyclin D/CDK4. Nature *366*, 704–707.

Sherr, C., and Roberts, J. (1995). Inhibitors of mammalian G1 cyclin-dependent kinases. Genes Dev. *9*, 1149–1163.

Slingerland, J., Hengst, L., Pan, C., Alexander, D., Stampfer, M., and Reed, S. (1994). A novel inhibitor of cyclin-cdk activity detected in transforming growth factor β-arrested epithelial cells. Mol. Cell. Biol. *14*, 3683–3694.

Soriano, P., Montgomery, C., Geske, R., and Bradley, A. (1991). Targeted disruption of the c-*src* proto-oncogene leads to osteopetrosis in mice. Cell *64*, 693–702.

Toyoshima, H., and Hunter, T. (1994). p27, a novel inhibitor of G1 cyclin–Cdk protein kinase activity, is related to p21. Cell *78*, 67–74.

Tybulewicz, V.L., Crawford, C.E., Jackson, P.K., Bronson, R.T., and Mulligan, R.C. (1991). Neonatal lethality and lymphopenia in mice with a homozygous disruption of the c-*abl* proto-oncogene. Cell *65*, 1153–1163.

van Buul-Offers, S., Haan, K., Reijnen-Gresnigt, M., Meinsma, D., Jansen, M., Oei, S., Bonte, E., Sussenbach, J., and Van den Brande, J. (1995). Overexpression of human insulin-like growth factor II in transgenic mice causes increased growth of the thymus. J. Endocrinol. *144*, 491–502.

Waga, S., Hannon, G., Beach, D., and Stillman, B. (1994). The p21 inhibitor of cyclin-dependent kinases controls DNA replication by interaction with PCNA. Nature *369*, 574–578.

Ward, A., Bates, P., Fisher, R., Richardson, L., and Graham, C. (1994). Disproportionate growth in mice with Igf-2 transgenes. Proc. Natl. Acad. Sci. USA *91*, 10365–10369.

Williams, B.O., Schmitt, E.M., Remington, L., Bronson, R.T., Albert, D.M., Weinberg, R.A., and Jacks, T. (1994). Extensive contribution of Rb-deficient cells to adult chimeric mice with limited histopathological consequences. EMBO J. *13*, 4251–4259.

Wolf, E., Kramer, R., Blum, W., Foll, J., and Brem, G. (1994). Consequences of postnatally elevated insulin-like growth factor II in transgenic mice: endocrine changes and effects on body and organ growth. Endocrinology *135*, 1877–1886.

Xiong, Y., Hannon, G., Zhang, H., Casso, D., Kobayashi, R., and Beach, D. (1993a). p21 is a universal inhibitor of cyclin kinases. Nature *366*, 701–704.

Xiong, Y., Zhang, H., and Beach, D. (1993b). Subunit rearrangement of the cyclin-dependent kinases is associated with cellular transformation. Genes Dev. *7*, 1572–1583.